



## Review

# Quantifying heterogeneity in human tumours using MRI and PET

Marie-Claude Asselin<sup>a</sup>, James P.B. O'Connor<sup>a</sup>, Ronald Boellaard<sup>b</sup>, Neil A. Thacker<sup>a</sup>, Alan Jackson<sup>a,\*</sup>

<sup>a</sup> Wolfson Molecular Imaging Centre, University of Manchester, UK

<sup>b</sup> Department of PET Research, VU University Medical Center, Amsterdam, The Netherlands

Available online 20 January 2012

### KEYWORDS

Tumour  
Imaging  
Positron emission tomography  
Magnetic resonance imaging  
Heterogeneity

**Abstract** Most tumours, even those of the same histological type and grade, demonstrate considerable biological heterogeneity. Variations in genomic subtype, growth factor expression and local microenvironmental factors can result in regional variations within individual tumours. For example, localised variations in tumour cell proliferation, cell death, metabolic activity and vascular structure will be accompanied by variations in oxygenation status, pH and drug delivery that may directly affect therapeutic response. Documenting and quantifying regional heterogeneity within the tumour requires histological or imaging techniques. There is increasing evidence that quantitative imaging biomarkers can be used in vivo to provide important, reproducible and repeatable estimates of tumoural heterogeneity.

In this article we review the imaging methods available to provide appropriate biomarkers of tumour structure and function. We also discuss the significant technical issues involved in the quantitative estimation of heterogeneity and the range of descriptive metrics that can be derived. Finally, we have reviewed the existing clinical evidence that heterogeneity metrics provide additional useful information in drug discovery and development and in clinical practice.

© 2012 Elsevier Ltd. All rights reserved.

## 1. The significance of tumour heterogeneity

Most tumours demonstrate biological heterogeneity<sup>1–3</sup> including heterogeneity in genomic subtypes, variations in the expression of growth factors and pro and anti-angiogenic factors<sup>4–9</sup> and variations in the tumoural

microenvironment. These can present as differences between tumours in different individuals. For example, O<sup>6</sup>-methylguanine-DNA methyltransferase, a DNA repair enzyme, is silenced by methylation of the gene promoter in 50% of glioblastoma (GBM), contributing to chemosensitivity, and improved survival.<sup>10</sup>

Heterogeneity also occurs within individual tumours with regional variations in proliferation, cell death, metabolic activity, vascular structure and other factors. Increasingly there is also recognition that relapse and metastatic behaviour result to a large extent from cancer

\* Corresponding author. Address: Wolfson Molecular Imaging Centre, 27 Palatine Rd., Withington, Manchester M20 3LJ, UK. Tel.: +44 161 275 0040; fax: +44 161 275 0003.

E-mail address: [alan.jackson@manchester.ac.uk](mailto:alan.jackson@manchester.ac.uk) (A. Jackson).

stem cells which exist in distinct micro-environmental niches.<sup>11–14</sup>

Experimental evidence has shown that vascular heterogeneity can be associated with disease progression, therapeutic response and malignancy.<sup>15,16</sup> Despite this, information concerning heterogeneity is rarely utilised even in imaging based studies and there is no consensus concerning the choice of descriptive metrics.<sup>17,18</sup>

## 2. Studying and quantifying tumour heterogeneity with imaging biomarkers (IB)

Studying heterogeneity within solid tumours requires histological<sup>19–22</sup> or imaging data.<sup>17,23</sup> Histological biomarkers offer high spatial resolution and biological specificity but are difficult to localise, subject to sampling errors and can seldom be repeated. Imaging biomarkers can provide spatial information, are minimal or non-invasive and can be repeated.<sup>24–26</sup> Modern imaging systems produce digital data but the development of IB requires the development and validation of acquisition and analysis techniques.

### 2.1. Magnetic Resonance Imaging (MRI) biomarkers

There has been particular interest in the use of diffusion weighted imaging (DWI) and dynamic contrast enhanced MRI (DCE-MRI). Other MRI IB such as magnetisation transfer contrast imaging, arterial spin labelling and novel targeted MRI contrast agents have yet to find widespread application.<sup>27</sup>

DWI sensitises MRI to water diffusion within the extravascular extracellular space (EES) and is affected by the size and configuration of the cellular population. Quantitative metrics reflect freedom of diffusion (ADC (Apparent Diffusional Coefficient)) and the magnitude of anisotropy, e.g. FA (Fractional Anisotropy). Preclinical and clinical data show that DWI can be used to assess regional cellularity, aggressiveness, to predict suitable therapies and monitor response.<sup>28,29</sup>

DCE-MRI uses dynamic acquisition of images during and after the injection of intravenous contrast agent.<sup>30,31</sup> Signal changes can be transformed to absolute concentration of contrast allowing analysis using pharmacokinetic models. Measured parameters typically include vascular fraction ( $v_p$ ), size of the EES ( $v_e$ ) and contrast transfer coefficient ( $K^{trans}$ ). DCE-MRI has been widely employed in early phase trials of antiangiogenic and vascular disrupting therapies. Although DCE-MRI requires the injection of intravenous contrast this does not limit repeated examinations.

### 2.2. Positron emission tomography (PET) biomarkers

PET provides unique biological specificity, allowing dynamic or static imaging of biological molecules

labelled with positron emitting isotopes (e.g.  $^{15}\text{O}$ ,  $^{18}\text{F}$ ,  $^{11}\text{C}$ ). The technique is associated with a significant radiation dose, which limits repeated measurements, especially when used in combination with computer tomography (CT). Nonetheless, experimental designs with repeated examinations and/or imaging with multiple radiotracers is possible. The most widely used PET tracer in oncology is fluoro-2-deoxy-D-glucose (FDG) radiolabelled with  $^{18}\text{F}$ . FDG follows the same initial metabolic pathway as glucose but, after conversion by hexokinase, its metabolite FDG-6-phosphate becomes trapped in cells at a rate proportional to that of glucose utilisation. In cancer cells glycolysis is elevated and FDG uptake is increased. Following administration the time course of radioactivity in tissues reflects the transport of the radiotracer and enzymatic activity, either of which may be altered. When an input function is available, the rate constants describing these processes can be estimated using a kinetic model and combined to give the influx rate constant ( $K_i$ ). Alternatively, radioactivity can be measured over a fixed period at a given time following administration and normalised to yield a standard uptake value (SUV). Some of the other radiotracers in use for oncologic applications include [ $^{15}\text{O}$ ]H<sub>2</sub>O for the measurement of blood perfusion, [ $^{18}\text{F}$ ]3'-deoxy-3'-fluorothymidine (FLT) for cellular proliferation and [ $^{18}\text{F}$ ]fluoromisonidazole (FMISO) for hypoxia. Several anti-cancer drugs have also been radiolabelled and their distribution imaged by PET.

## 3. Technical considerations

### 3.1. Impact of data quality

Unfortunately, data from individual voxels will vary in the signal-to-noise ratio so that the confidence limits on the calculation of a parameter will vary across the parametric map. It is important to realise that an analysis of heterogeneity patterns must take into account potential inaccuracies in the calculation of individual pixel values which may require labelling some pixels as un-analysable or deriving parameters that allow direct estimation of the confidence limits.<sup>18,32</sup> Assessments of heterogeneity should therefore take such correlations into account via the use of the appropriate Mahalanobis distance measures, or equivalent.

Heterogeneity analysis of PET images is further confounded by partial volume effects due to the limited spatial resolution and high noise level. In their simulation study, van Velden et al.<sup>65</sup> denoised (using an edge-preserving bilateral filter) and corrected the heterogeneous tumours for partial volume (using van Cittert deconvolution with Gibbs priors) improving the accuracy of the heterogeneity metric derived from the area under the curve (AUC) of cumulative intensity–volume histograms. Other heterogeneity metrics are likely to be more

sensitive to these effects. In addition to post-processing the reconstructed images, the image reconstruction parameters impact on noise and spatial resolution and influence the reliability of certain heterogeneity metrics more than others.<sup>33</sup> The level (whole tumour, subregions or voxel) at which heterogeneity analyses can reliably be performed is also limited by motion and co-registration for longitudinal studies and multi-tracers and/or multi-modality studies. Radiotracer uptake heterogeneity has been shown to impact tumour delineation, the extent of which depends on the segmentation method.<sup>34</sup> Conversely, tumour delineation will influence heterogeneity metrics, with some being more sensitive to boundaries than others, e.g. cumulative histogram (Fig. 1).<sup>35</sup>

## 4. Methods for quantifying heterogeneity

### 4.1. Use of selective regions of interest (ROI)

Manual selection of small regions of interest with high/low values has been used for both DWI and DCE-MRI data.<sup>36–40</sup> The technique is simple and inter-observer variations may be of minimal importance where large variations are present. However, this approach is not recommended for therapeutic trials or treatment monitoring.<sup>41</sup> Subjective or semi-quantitative methods for grading the severity of heterogeneity have also been proposed but show significant<sup>42</sup> inter-observer variations and poor reproducibility.<sup>43–45</sup>

Rim enhancement patterns led to a quantitative approach to describe radial heterogeneity on MR<sup>46,47</sup> where the tumour is divided into concentric circles and mean or median parameter values plotted against band number. This has been widely used in animal stud-

ies,<sup>48,49</sup> but cannot be applied when heterogeneity patterns are not radial, which is often the case in human tumours.

At the limited spatial resolution of PET images, homogeneous radiotracer uptake in an ellipsoid would appear to progressively decline away from the centre and the deviation from this model has been used to quantify heterogeneity in FDG uptake<sup>50</sup> and found to be a predictor of outcome in 234 sarcoma patients.<sup>51</sup>

### 4.2. Cluster analysis

Cluster analysis is attractive since it will, in theory, allow identification of tumour components with common properties. It also maintains information regarding spatial relationships of tissue subtypes. Cluster analysis has been used in a small number of animal studies but has yet to be applied in human MR data.<sup>52,53</sup>

In a multi-imaging biomarker study,<sup>54</sup> 13 cancer patients underwent DCE-MRI for the estimation of blood volume and blood flow, static FDG PET for the measurement of glucose metabolism and static [<sup>18</sup>F]-galacto-RGD (arginine-glycine-aspartate) for imaging the  $\alpha_v\beta_{3/5}$  integrin receptors. After delineating the whole tumour on the fused PET images, the distribution of SUVs at the voxel level were clustered into four regions using preset thresholds for the two tracers on a scatter-plot: high FDG and RGD, high FDG and low RGD, low FDG and high RGD and low FDG and RGD. Significant differences in blood volume but not blood flow were detected between regions of both high glucose metabolism and  $\alpha_v\beta_{3/5}$  expression and regions of both low glucose metabolism and  $\alpha_v\beta_{3/5}$  expression. No significant correlation was found between the MR and

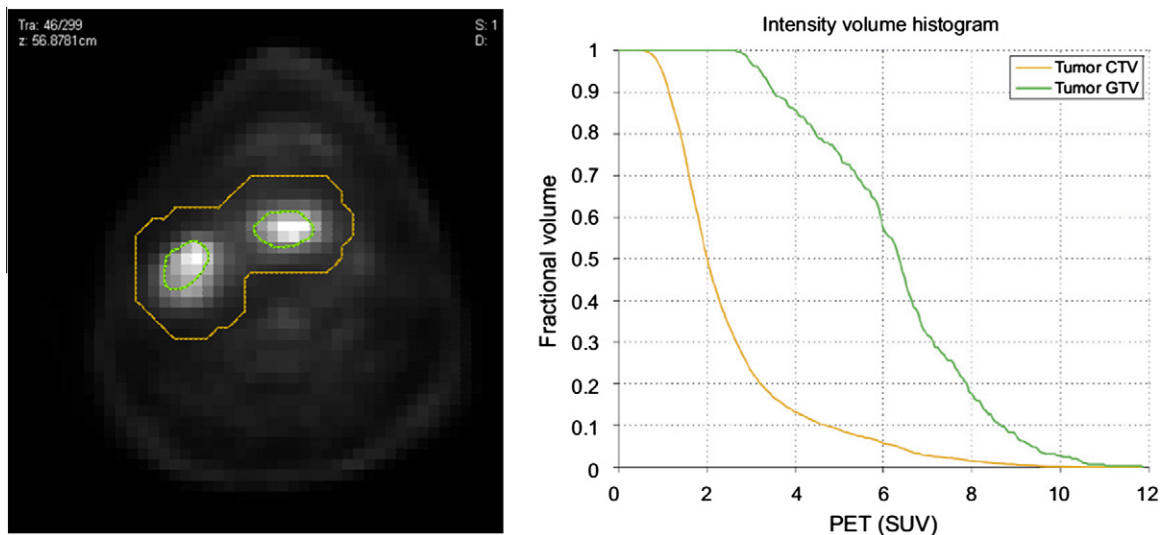


Fig. 1. Pre-treatment FDG scan of the head and neck cancer showing different tumour delineations are representing clinical (brown) and gross (green) tumour volume (Left). Intensity-volume histograms showing the difference depending on the choice of region of interest (right). (Adapted from<sup>35</sup> with permission).

PET biomarkers when the tumours were analysed as a whole.

#### 4.3. Selective classification

One simple method is to measure the fraction of pixels that enhance after contrast administration (EnF (enhancing fraction)). EnF has been shown to support differentiation between, and to predict formal measurements of  $v_p$  and  $K^{trans}$  in low and high grade glioma.<sup>55,56</sup> EnF provided predictive information in ovarian, cervical and colorectal cancers<sup>16,57,58</sup> and a phase I trial of CNTO 95 showed that enhancing fraction can predict stable and progressive disease in the absence of clear treatment effects.<sup>59</sup>

#### 4.4. Histogram analysis

The intensity histogram allows a range of descriptive parameters including: range, mean, median, standard deviation (SD), skewness, kurtosis, entropy and various percentile cut-off values.<sup>46,60–63</sup> A growing number of studies demonstrate important changes in response to treatment using histogram analysis that were not seen on whole tumour measurements.<sup>46,64</sup> It must be realised that all information concerning spatial relationships within the tumour is lost. El Naqa et al.<sup>35</sup> introduced the cumulative intensity–volume histogram in which the volume is plotted as a function of image intensity that is equal to or higher than a certain value and from which various metrics can be extracted, e.g. percentage volume having at least a given percentage intensity. van Velden et al.<sup>65</sup> assessed the AUC of this plot as the quantitative index of uptake heterogeneity in simulated tumours and static FDG images. Although this heterogeneity metric characterised a rim pattern, it appeared less sensitive to heterogeneous radiotracer distribution and to a heterogeneous response than the simpler inverse of the coefficient of variation (mean/SD).

#### 4.5. Texture mapping

Textural analysis provides a method to re-introduce spatial information. The available techniques include grey-level spatial co-occurrence matrices, and convolution based area representation (such as Gabor and Wavelet filters). Co-occurrence matrices measure the probability of finding a voxel with some grey level value at specific relative angle and distances. These can then be used to calculate a number of textural characteristics, including “contrast” and “entropy” (Fig. 2).

Texture analysis has been used in breast cancer to improve distinction between benign and malignant lesions.<sup>66,67</sup> It has the disadvantage that the simplicity of derived parameters results in responses that are counter-intuitive with regard to the underlying variation in

tumour structure. El Naqa et al.<sup>35</sup> were among the first to explore textural features in static FDG images to predict treatment outcome. The combination of texture energy with the intensity–volume histogram was found to predict disease persistence in 14 patients with cervix cancer whereas overall survival in nine patients with head and neck cancer could be predicted with excellent power by combining shape extent with the intensity–volume histogram. Tixier et al.<sup>68</sup> compared global (distribution histogram), regional (intensity–size zone matrix) and local (co-occurrence matrix) features on static FDG images for their capacity to classify 41 patients with oesophageal cancer with respect to response to chemoradiotherapy and showed that local homogeneity and entropy as well as regional intensity and size–zone variabilities could identify non-responders, partial and complete responders with higher sensitivity than SUV measurements (Fig. 2).

#### 4.6. Spatial geometric approaches

Here individual parameters are interpreted as the height on an extruded 4D hypervolume. Geometric features like surface area, volume, surface to volume ratio and box-count fractal dimension can be calculated and used as quantitative descriptors of heterogeneity.<sup>18,69</sup> Clinical studies show increased discriminative power between low-grade and high-grade glioma and increased ability to predict outcome in colorectal metastatic disease in response to bevacizumab.<sup>16</sup> Dimitrakopoulou-Strauss et al.<sup>70</sup> first used the box-counting method on time–activity curves from dynamic FDG, [<sup>15</sup>O]H<sub>2</sub>O and 6-[<sup>18</sup>F]fluoro-L-DOPA (as a potential radiotracer for melanin synthesis) images from 11 metastatic melanoma patients, and did not find evidence of heterogeneous distribution within the manually delineated lesions. However, when combined with SUVs and kinetic parameters in discriminant analysis, fractal dimension improved the differentiation of sarcomas from dynamic FDG images.<sup>71</sup>

### 5. Clinical evidence for value of heterogeneity metrics

Increasing numbers of clinical studies demonstrate the ability of heterogeneity metrics to provide additional, important information relating to tumour phenotype, therapeutic response and prognosis.

#### 5.1. Heterogeneity in DWI metrics

Early studies in glioma showed that mean values of [ADC] were less clinically relevant than the minimum values (minADC). A negative correlation between minADC and Ki-67 has been demonstrated in high-grade glioma and the use of a minADC cutoff value of 0.009 mm<sup>2</sup>/s for the differentiation between high and



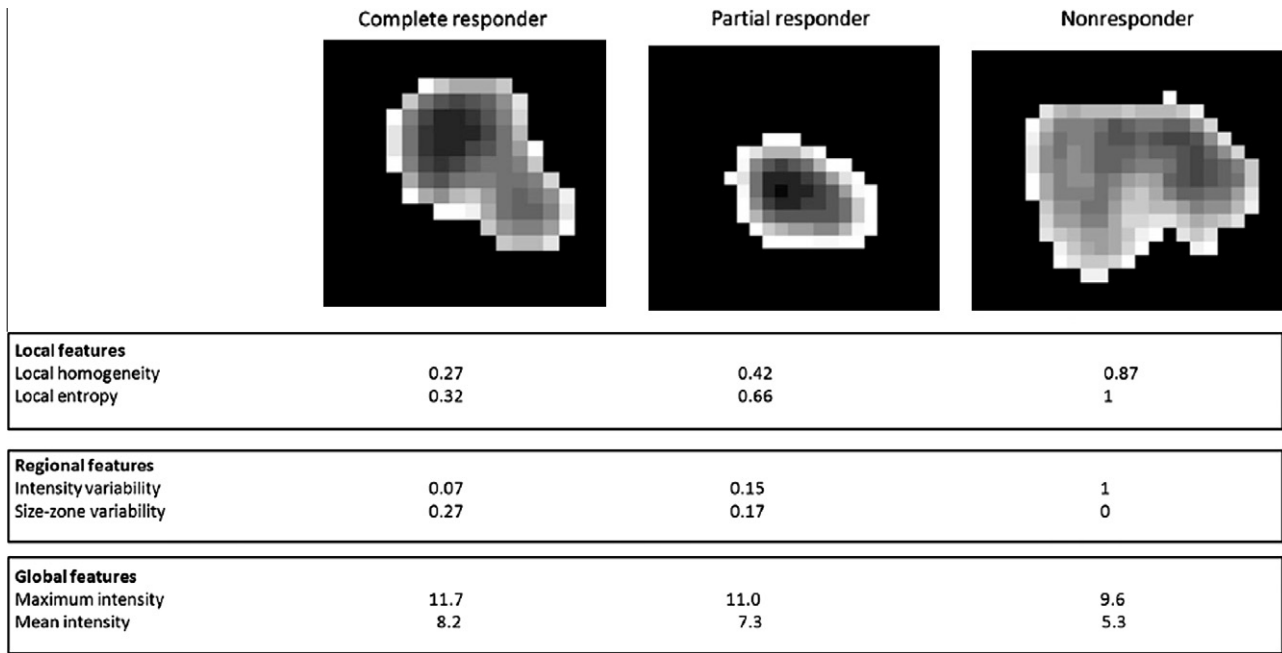


Fig. 2. Examples of textural features extracted from baseline  $^{18}\text{F}$ -FDG PET images in patients with oesophageal cancer showing variations in textural features between complete responders, partial responders and non-responders. (Adapted from<sup>68</sup> with permission).

low-grade neuroepithelial tumours provided the best combination of sensitivity (85.4%) and specificity (71.0%).<sup>38</sup> These low values of ADC are believed to reflect hyper-cellular areas where proliferation is high and the size of the EES consequently reduced.

### 5.2. Detecting and predicting treatment response with DWI heterogeneity metrics

The distribution of pre-treatment ADC values in glioblastoma predicted progression free survival with bevacizumab therapy and optimal separation was obtained by use of a cut-off value derived from distribution histograms.<sup>72</sup> Researchers from the University of Michigan spatially registered pretreatment to early post treatment maps of ADC and demonstrated that although mean values of ADC in tumours showed no predictive value, the presence of significant numbers of pixels showing early changes in ADC values was highly predictive.<sup>73–75</sup> This approach, labelled the parametric response map (prm; vide infra), is being increasingly adopted in studies of cerebral tumours. However, prm is invalidated by the treatment induced spatial distortion restricting its application in extra-cerebral tumours.

Clinical evidence for DWI heterogeneity measures has also been demonstrated in extra-cranial tumours. In 12 patients with 48 metastatic liver lesions from colorectal cancer, positive correlations were observed between minADC and reduction ratio in response to arterial infusion chemotherapy with 5-fluorouracil.<sup>76</sup> A study of minADC and prognosis in endometrial cancer found correlations between minADC of the primary tumour and FIGO stage ( $P = 0.001$ ), depth of myome-

trial invasion ( $P < 0.001$ ), cervical involvement ( $P = 0.003$ ), lymph node metastasis ( $P = 0.027$ ), ovarian metastasis ( $P < 0.001$ ), peritoneal cytology ( $P = 0.027$ ) and tumour maximum size ( $P < 0.001$ ). A low minADC was also associated with reduced survival ( $P < 0.001$ ) and ADCmin was an independent factor for disease recurrence ( $P = 0.019$ ).<sup>37</sup> A further study in endometrial cancer concluded that quartile ADC had a strong relationship with the invasiveness of endometrial carcinomas, while mean ADC value did not.<sup>77</sup>

### 5.3. Heterogeneity in DCE-MRI metrics

Peripheral contrast enhancement is a common feature of aggressive tumours and, in the breast, is used as a diagnostic indicator of malignancy.<sup>15</sup> Heterogeneity in vascular features has been associated with decreased survival, poor therapeutic response and increased metastatic potential in a range of systemic tumour types.<sup>12,62,78,79</sup>

### 5.4. Detecting and predicting treatment response with DCE-MRI heterogeneity metrics

An early study of high-grade glioma showed that the 95th percentile of the distribution of  $K^{\text{trans}}$  predicted overall survival whilst median values did not.<sup>80</sup> Galban and colleagues applied the prm technique to DCE-MRI<sup>81</sup> showing that direct pixel-by-pixel comparison of CBV values from images acquired before and one and three weeks after therapy provided more accurate prediction of survival than overall percentage change.

In breast cancer patients, receiving cytotoxic chemotherapy for locally advanced disease, the SD

and kurtosis of enhancement amplitude before therapy predicted subsequent radiological response. Furthermore, tumours that responded had a significant reduction in the SD of enhancement amplitude and showed a change from a heterogeneous distribution into a more homogeneous one.<sup>82</sup> In a similar study, patients surviving for more than five years were found to have a significantly less heterogeneous distribution of relative signal intensity (RSI) in the baseline DCE-MRI distribution than non-survivors.<sup>83</sup> Padhani et al. found that changes in vascular heterogeneity quantified by the range of  $K^{\text{trans}}$  distributions at the end of cycle two were predictive of both clinical and histopathologic responses after three to six cycles of therapy.<sup>84</sup>

The 10th percentile of the distribution of relative signal intensity was found to better predict tumour recurrence after radiotherapy in patients with cervical carcinoma than mean or median values.<sup>45</sup> A more recent study quantified heterogeneity using the percentiles of voxel signal intensities in the plateau phase of enhancement curves. Low values of the 5th to 20th percentiles were correlated with poor primary tumour control and short disease-free survival. The 5th percentile measured at two weeks of therapy provided the best prediction for eight-year primary tumour control.<sup>85</sup>

In colorectal cancer, a study of 10 patients with 26 colorectal cancer liver metastases treated with bevacizumab and FOLFOX6 demonstrated that 86% of the variance in post treatment shrinkage could be explained by a model combining baseline measurements of  $v_e$ , tumour enhancing fraction (EnF), and microvascular uniformity ( $R^2 = 0.86$ ,  $P < 0.00005$ ).<sup>16</sup>

### 5.5. DCE-MRI heterogeneity metrics in clinical applications

Early work with T2\* based DCE-MRI in brain tumours described a close relationship between grade and cerebral blood volume (CBV).<sup>39,40</sup> Subsequently, the use of parametric maps combined with image guided biopsy, has become a common clinical practice.<sup>86</sup> Similarly, evidence that regional increases in CBV precede other indicators of malignant dedifferentiation in low-grade glioma has led to the introduction of DCE-MRI in surveillance protocols.<sup>87</sup>

Considerable evidence of the clinical value of heterogeneity metrics has also accrued in breast cancer imaging. Early work demonstrated that measurements of SD of parameters such as  $K^{\text{trans}}$  within a ROI significantly improve diagnostic accuracy when attempting to distinguish malignant from benign lesions.<sup>60</sup> Heterogeneity of enhancement patterns are now included in the ACR Breast Imaging-Reporting and Data System (BI-RADS) MRI lexicon.<sup>15</sup>

### 5.6. Heterogeneity in PET metrics

The majority of heterogeneity analyses have been performed on static images since they are more widely available than dynamic images and less noisy than parametric maps. However, SUVs are kinetically heterogeneous, being influenced by transport and trapping mechanisms. Kinetic modelling of dynamic scans may be required when comparing heterogeneity of different biomarkers if one is to interpret the differences between different modalities and/or multiple radiotracers<sup>54</sup> and take full advantage of the specificity of PET.

### 5.7. Detecting and predicting treatment response with PET heterogeneity metrics

In a large cohort of 234 sarcoma patients before neoadjuvant chemotherapy or surgical resection, the heterogeneity metric defined as the percentage of variability in voxelwise FDG uptake that is not explained by an ellipsoidal pattern was a stronger independent predictor of survival than SUV.<sup>51</sup> Tumours with highly heterogeneous metabolism likely have a high metastatic potential associated with poor patient outcome. However, there was only a weak association of the heterogeneity metric with the presence of necrosis, the histological hallmark of high grade in this cancer on CT and MR images available for 77 of these patients.

Heterogeneity in radiotracer uptake holds the potential to be incorporated into treatment planning for radiotherapy. Individualisation of treatment for head and neck cancer based on hypoxia PET imaging with FMISO has recently been proposed and its clinical feasibility for intensity-modulated radiation therapy theoretically assessed.<sup>88</sup> Taking into consideration heterogeneity of hypoxic regions could contribute to the identification of patients who would benefit from a segmented dose escalation focused to the hypoxic target.

## 6. Summary and conclusions

Quantification of tumour heterogeneity has the potential to add valuable information to clinical imaging studies. The choice of metrics for heterogeneity is uncertain and may differ between applications. Moreover, the technical challenges of producing meaningful heterogeneity metrics are significant and, in particular, issues associated with variation in data quality must be addressed.

### Conflict of interest statement

None declared.

## Acknowledgements

The authors are members of the QuIC-ConCePT project partly funded by EFPIA companies and the Innovative Medicine Initiative Joint Undertaking (IMI JU) under Grant agreement number 115151.

QuIC-ConCePT Consortium participants include: AstraZeneca, European Organisation for Research and Treatment of Cancer (EORTC), Cancer Research United Kingdom (UK), University of Manchester, Westfälische Wilhelms-Universität Münster, Radboud University Nijmegen Medical Centre, Institut National de la Santé et de la Recherche Médicale, Stichting Maastricht Radiation Oncology 'Maastricht Clinic', VUmc Amsterdam, King's College London, Universitair Ziekenhuis Antwerpen, Institute of Cancer Research – Royal Cancer Hospital, Erasmus Universitair Medisch Centrum Rotterdam, Imperial College of Science Technology and Medicine, Keosys S.A.S., Eidgenössische Technische Hochschule Zürich, Amgen NV, Eli Lilly and Company Ltd, GlaxoSmithKline Research & Development Limited, Merck KGa, Pfizer Limited, F. Hoffmann – La Roche Ltd., Sanofi–Aventis Research and Development.

## References

- Weidner N, Semple JP, Welch WR, Folkman J. Tumour angiogenesis and metastasis – correlation in invasive breast carcinoma. *N Engl J Med* 1991;**324**(1):1–8, Research Support, Non-US Gov't Research Support, US Gov't, P.H.S.
- Schor AM, Pazouki S, Morris J, et al. Heterogeneity in microvascular density in lung tumours: comparison with normal bronchus. *Br J Cancer* 1998;**77**(6):946–51, Comparative Study Research Support, Non-US Gov't.
- Wyss MT, Hofer S, Hefti M, et al. Spatial heterogeneity of low-grade gliomas at the capillary level: a PET study on tumour blood flow and amino acid uptake. *J Nucl Med* 2007;**48**(7):1047–52, Research Support, Non-US Gov't.
- Heppner GH, Miller BE. Therapeutic implications of tumour heterogeneity. *Semin Oncol* 1989;**16**(2):91–105, Research Support, US Gov't, P.H.S. Review.
- Heppner GH, Chong YC, Fulton AM. Host-mediated induction of tumour heterogeneity. *Ann N Y Acad Sci* 1989;**567**:234–42, Research Support, Non-US Gov't Research Support, US Gov't, P.H.S. Review.
- Heppner G, Yamashina K, Miller B, Miller F. Tumour heterogeneity in metastasis. *Prog Clin Biol Res* 1986;**212**:45–59, Research Support, Non-US Gov't Research Support, US Gov't, P.H.S.
- Heppner GH. Tumour heterogeneity. *Cancer Res* 1984;**44**(6):2259–65, Research Support, Non-US Gov't Research Support, US Gov't, P.H.S. Review.
- Shipitsin M, Campbell LL, Argani P, et al. Molecular definition of breast tumour heterogeneity. *Cancer Cell* 2007;**11**(3):259–73, Research Support, N.I.H., Extramural Research Support, Non-US Gov't Research Support, US Gov't, Non-P.H.S.
- Carmeliet P, Jain RK. Angiogenesis in cancer and other diseases. *Nature* 2000;**407**(6801):249–57, Research Support, Non-US Gov't Research Support, US Gov't, Non-P.H.S. Research Support, US Gov't, P.H.S. Review.
- Mollemann M, Wolter M, Felsberg J, Collins VP, Reifemberger G. Frequent promoter hypermethylation and low expression of the MGMT gene in oligodendroglial tumours. *Int J Cancer* 2005;**113**(3):379–85, Research Support, Non-US Gov't.
- Parsa AT, Wachhorst S, Lamborn KR, et al. Prognostic significance of intracranial dissemination of glioblastoma multiforme in adults. *J Neurosurg* 2005;**102**(4):622–8, Research Support, US Gov't, P.H.S.
- Chuthapath S, Eremin J, El-Sheemey M, Eremin O. Breast cancer chemoresistance: emerging importance of cancer stem cells. *Surg Oncol* 2010;**19**(1):27–32, Review.
- Gilbertson RJ, Rich JN. Making a tumour's bed: glioblastoma stem cells and the vascular niche. *Nat Rev Cancer* 2007;**7**(10):733–6, Research Support, N.I.H., Extramural Research Support, Non-US Gov't Review.
- Sneddon JB, Werb Z. Location, location, location: the cancer stem cell niche. *Cell Stem Cell* 2007;**1**(6):607–11, Research Support, N.I.H., Extramural Research Support, Non-US Gov't Review.
- Agrawal G, Su MY, Nalcioglu O, Feig SA, Chen JH. Significance of breast lesion descriptors in the ACR BI-RADS MRI lexicon. *Cancer* 2009;**115**(7):1363–80, Research Support, N.I.H., Extramural Research Support, Non-US Gov't.
- O'Connor JP, Rose CJ, Jackson A, et al. DCE-MRI biomarkers of tumour heterogeneity predict CRC liver metastasis shrinkage following bevacizumab and FOLFOX-6. *Br J Cancer* 2011;**105**(1):139–45, Research Support, Non-US Gov't.
- Jackson A, O'Connor JP, Parker GJ, Jayson GC. Imaging tumour vascular heterogeneity and angiogenesis using dynamic contrast-enhanced magnetic resonance imaging. *Clin Cancer Res* 2007;**13**(12):3449–59, Research Support, Non-US Gov't, Review.
- Rose CJ, Mills SJ, O'Connor JP, et al. Quantifying spatial heterogeneity in dynamic contrast-enhanced MRI parameter maps. *Magn Reson Med* 2009;**62**(2):488–99, Research Support, Non-US Gov't.
- Yaromina A, Holscher T, Eicheler W, et al. Does heterogeneity of pimonidazole labelling correspond to the heterogeneity of radiation-response of FaDu human squamous cell carcinoma? *Radiother Oncol* 2005;**76**(2):206–12, Research Support, Non-US Gov't.
- Diwakar N, Sperandio M, Sherriff M, Brown A, Odell EW. Heterogeneity, histological features and DNA ploidy in oral carcinoma by image-based analysis. *Oral Oncol* 2005;**41**(4):416–22, Research Support, Non-US Gov't.
- Iglesias-Rozas JR, Hopf N. Histological heterogeneity of human glioblastomas investigated with an unsupervised neural network (SOM). *Histol Histopathol* 2005;**20**(2):351–6.
- Sharifi-Salamatian V, Pesquet-Popescu B, Simony-Lafontaine J, Rigaut JP. Index for spatial heterogeneity in breast cancer. *J Microsc* 2004;**216**(Pt. 2):110–22, Comparative Study.
- Yang X, Knopp MV. Quantifying tumour vascular heterogeneity with dynamic contrast-enhanced magnetic resonance imaging: a review. *J Biomed Biotechnol* 2011;**2011**:732848, Research Support, Non-US Gov't Review.
- Finley Austin MJ, Babiss L. Commentary: where and how could biomarkers be used in 2016? *AAPS J* 2006;**8**(1):E185–9.
- Tesch G, Amur S, Schousboe JT, et al. Successes achieved and challenges ahead in translating biomarkers into clinical applications. *AAPS J* 2010;**12**(3):243–53.
- Amur S, Frueh FW, Lesko LJ, Huang SM. Integration and use of biomarkers in drug development, regulation and clinical practice: a US regulatory perspective. *Biomark Med* 2008;**2**(3):305–11.
- Yankeelov TE, Arlinghaus LR, Li X, Gore JC. The role of magnetic resonance imaging biomarkers in clinical trials of treatment response in cancer. *Semin Oncol* 2011;**38**(1):16–25, Research Support, N.I.H., Extramural Review.
- Padhani AR, Liu G, Koh DM, et al. Diffusion-weighted magnetic resonance imaging as a cancer biomarker: consensus and recommendations. *Neoplasia* 2009;**11**(2):102–25, Consensus Development Conference, NIH.

29. Padhani AR. Diffusion magnetic resonance imaging in cancer patient management. *Semin Radiat Oncol* 2011;**21**(2):119–40, Review.
30. O'Connor JP, Jackson A, Parker GJ, Jayson GC. DCE-MRI biomarkers in the clinical evaluation of antiangiogenic and vascular disrupting agents. *Br J Cancer* 2007;**96**(2):189–95, Research Support, Non-US Gov't Review.
31. Jackson A. Analysis of dynamic contrast enhanced MRI. *Br J Radiol* 2004;**77**(Spec No. 2):S154–66, Review.
32. Li KL, Zhu XP, Jackson A. Parametric mapping of scaled fitting error in dynamic susceptibility contrast enhanced MR perfusion imaging. *Br J Radiol* 2000;**73**(869):470–81, Research Support, Non-US Gov't.
33. Galavis PE, Hollensen C, Jallow N, Paliwal B, Jeraj R. Variability of textural features in FDG PET images due to different acquisition modes and reconstruction parameters. *Acta Oncologica* 2010;**49**(7):1012–6, Evaluation Studies Research Support, N.I.H., Extramural Research Support, Non-US Gov't.
34. Hatt M, Cheze-le Rest C, van Baardwijk A, et al. Impact of tumour size and tracer uptake heterogeneity in 18F-FDG PET and CT non-small cell lung cancer tumour delineation. *J Nucl Med* 2011;**52**(11):1690–7.
35. El Naqa I, Grigsby P, Apte A, et al. Exploring feature-based approaches in PET images for predicting cancer treatment outcomes. *Pattern Recogn* 2009;**42**(6):1162–71.
36. Duygulu G, Ovali GY, Calli C, et al. Intracerebral metastasis showing restricted diffusion: correlation with histopathologic findings. *Eur J Radiol* 2010;**74**(1):117–20.
37. Nakamura K, Imafuku N, Nishida T, et al. Measurement of the minimum apparent diffusion coefficient (ADC<sub>min</sub>) of the primary tumour and CA125 are predictive of disease recurrence for patients with endometrial cancer. *Gynecol Oncol* 2011. doi:10.1016/j.ygyno.2011.10.014.
38. Chen Z, Ma L, Lou X, Zhou Z. Diagnostic value of minimum apparent diffusion coefficient values in prediction of neuroepithelial tumour grading. *J Magn Reson Imaging* 2010;**31**(6):1331–8.
39. Aronen HJ, Gazit IE, Louis DN, et al. Cerebral blood volume maps of gliomas: comparison with tumour grade and histologic findings. *Radiology* 1994;**191**(1):41–51, Comparative Study Research Support, Non-US Gov't Research Support, US Gov't, P.H.S.
40. Aronen HJ, Perkio J. Dynamic susceptibility contrast MRI of gliomas. *Neuroimaging Clin N Am* 2002;**12**(4):501–23, Research Support, Non-US Gov't Review.
41. Leach MO, Brindle KM, Evelhoch JL, et al. The assessment of antiangiogenic and antivascular therapies in early-stage clinical trials using magnetic resonance imaging: issues and recommendations. *Br J Cancer* 2005;**92**(9):1599–610, Guideline Research Support, Non-US Gov't.
42. Giesel FL, Choyke PL, Mehndiratta A, et al. Pharmacokinetic analysis of malignant pleural mesothelioma-initial results of tumour microcirculation and its correlation to microvessel density (CD-34). *Acad Radiol* 2008;**15**(5):563–70.
43. Mussurakis S, Buckley DL, Coady AM, Turnbull LW, Horsman A. Observer variability in the interpretation of contrast enhanced MRI of the breast. *Br J Radiol* 1996;**69**(827):1009–16, Clinical Trial Research Support, Non-US Gov't.
44. Borland D, Taylor 2nd MR. Rainbow color map (still) considered harmful. *IEEE Comput Graph Appl* 2007;**27**(2):14–7, Review.
45. Mayr NA, Yuh WT, Arnholt JC, et al. Pixel analysis of MR perfusion imaging in predicting radiation therapy outcome in cervical cancer. *J Magn Reson Imaging* 2000;**12**(6):1027–33.
46. Checkley D, Tessier JJ, Kendrew J, Waterton JC, Wedge SR. Use of dynamic contrast-enhanced MRI to evaluate acute treatment with ZD6474, a VEGF signalling inhibitor, in PC-3 prostate tumours. *Br J Cancer* 2003;**89**(10):1889–95.
47. Benjaminsen IC, Graff BA, Brurberg KG, Rofstad EK. Assessment of tumour blood perfusion by high-resolution dynamic contrast-enhanced MRI: a preclinical study of human melanoma xenografts. *Magn Reson Med* 2004;**52**(2):269–76, Research Support, Non-US Gov't.
48. Benjaminsen IC, Brurberg KG, Ruud EB, Rofstad EK. Assessment of extravascular extracellular space fraction in human melanoma xenografts by DCE-MRI and kinetic modelling. *Magn Reson Imaging* 2008;**26**(2):160–70.
49. Graff BA, Benjaminsen IC, Brurberg KG, Ruud EB, Rofstad EK. Comparison of tumour blood perfusion assessed by dynamic contrast-enhanced MRI with tumour blood supply assessed by invasive imaging. *J Magn Reson Imaging* 2005;**21**(3):272–81, Comparative Study Evaluation Studies Research Support, Non-US Gov't.
50. O'Sullivan F, Roy S, Eary J. A statistical measure of tissue heterogeneity with application to 3D PET sarcoma data. *Biostatistics* 2003;**4**(3):433–48, Research Support, Non-US Gov't Research Support, US Gov't, P.H.S.
51. Eary JF, O'Sullivan F, O'Sullivan J, Conrad EU. Spatial heterogeneity in sarcoma 18F-FDG uptake as a predictor of patient outcome. *J Nucl Med* 2008;**49**(12):1973–9, Research Support, N.I.H., Extramural.
52. Baudelet C, Gallez B. Cluster analysis of BOLD fMRI time series in tumours to study the heterogeneity of hemodynamic response to treatment. *Magn Reson Med* 2003;**49**(6):985–90, Evaluation Studies Research Support, Non-US Gov't.
53. Carano RA, Ross AL, Ross J, et al. Quantification of tumour tissue populations by multispectral analysis. *Magn Reson Med* 2004;**51**(3):542–51.
54. Metz S, Ganter C, Lorenzen S, et al. Phenotyping of tumour biology in patients by multimodality multiparametric imaging: relationship of microcirculation, alphavbeta3 expression, and glucose metabolism. *J Nucl Med* 2010;**51**(11):1691–8, Research Support, Non-US Gov't.
55. Mills SJ, Soh C, O'Connor JP, et al. Tumour enhancing fraction (EnF) in glioma: relationship to tumour grade. *Eur Radiol* 2009;**19**(6):1489–98, Research Support, Non-US Gov't.
56. Mills SJ, Soh C, O'Connor JP, et al. Enhancing fraction in glioma and its relationship to the tumoural vascular microenvironment: A dynamic contrast-enhanced MR imaging study. *AJNR Am J Neuroradiol* 2010;**31**(4):726–31, Research Support, Non-US Gov't.
57. Donaldson SB, Buckley DL, O'Connor JP, et al. Enhancing fraction measured using dynamic contrast-enhanced MRI predicts disease-free survival in patients with carcinoma of the cervix. *Br J Cancer* 2010;**102**(1):23–6, Evaluation Studies Research Support, Non-US Gov't.
58. O'Connor JP, Jayson GC, Jackson A, et al. Enhancing fraction predicts clinical outcome following first-line chemotherapy in patients with epithelial ovarian carcinoma. *Clin Cancer Res* 2007;**13**(20):6130–5, Research Support, Non-US Gov't.
59. Mullaitha SA, Ton NC, Parker GJ, et al. Phase I evaluation of a fully human anti-alpha<sub>v</sub> integrin monoclonal antibody (CNO 95) in patients with advanced solid tumours. *Clin Cancer Res* 2007;**13**(7):2128–35, Clinical Trial, Phase I Research Support, Non-US Gov't.
60. Issa B, Buckley DL, Turnbull LW. Heterogeneity analysis of Gd-DTPA uptake: improvement in breast lesion differentiation. *J Comput Assist Tomogr* 1999;**23**(4):615–21, Research Support, Non-US Gov't.
61. Ertas G, Gulcur HO, Tunaci M. Improved lesion detection in MR mammography: three-dimensional segmentation, moving voxel sampling, and normalised maximum intensity–time ratio entropy. *Acad Radiol* 2007;**14**(2):151–61.
62. Jackson A, Kassner A, Annesley-Williams D, et al. Abnormalities in the recirculation phase of contrast agent bolus passage in cerebral gliomas: comparison with relative blood volume and tumour grade. *AJNR Am J Neuroradiol* 2002;**23**(1):7–14.
63. Checkley D, Tessier JJ, Wedge SR, et al. Dynamic contrast-enhanced MRI of vascular changes induced by the VEGF-signalling



- inhibitor ZD4190 in human tumour xenografts. *Magn Reson Imaging* 2003;**21**(5):475–82.
64. O'Connor E, Fieller N, Holmes A, Waterton JC. How to analyse dynamic MRI in oncology; advanced histogram analysis gives better statistical power & insight than simple averaging. *Proc Int Soc Magn Reson Med* 2005;**13**:2101–5.
  65. van Velden FH, Cheebsumon P, Yaqub M, et al. Evaluation of a cumulative SUV–volume histogram method for parameterizing heterogeneous intratumoural FDG uptake in non-small cell lung cancer PET studies. *Eur J Nucl Med Mol Imaging* 2011;**38**(9):1636–47, Research Support, Non-US Gov't.
  66. Sinha S, Lucas-Quesada FA, DeBruhl ND, et al. Multifeature analysis of Gd-enhanced MR images of breast lesions. *J Magn Reson Imaging* 1997;**7**(6):1016–26.
  67. Chen W, Giger ML, Li H, Bick U, Newstead GM. Volumetric texture analysis of breast lesions on contrast-enhanced magnetic resonance images. *Magn Reson Med* 2007;**58**(3):562–71, Comparative Study Research Support, N.I.H., Extramural Research Support, Non-US Gov't Research Support, US Gov't, Non-P.H.S.
  68. Tixier F, Le Rest CC, Hatt M, et al. Intratumour heterogeneity characterised by textural features on baseline 18F-FDG PET images predicts response to concomitant radiochemotherapy in esophageal cancer. *J Nucl Med* 2011;**52**(3):369–78, Research Support, Non-US Gov't.
  69. Rose CJ, Mills S, O'Connor JP, et al. Quantifying heterogeneity in dynamic contrast-enhanced MRI parameter maps. *Med Image Comput Comput Assist Interv* 2007;**10**(Pt. 2):376–84.
  70. Dimitrakopoulou-Strauss A, Strauss LG, Burger C. Quantitative PET studies in pretreated melanoma patients: a comparison of 6-[18F]fluoro-L-dopa with 18F-FDG and (15)O-water using compartment and noncompartment analysis. *Journal of Nuclear Medicine: official publication, Society of Nuclear Medicine* 2001;**42**(2):248–56, Comparative Study.
  71. Dimitrakopoulou-Strauss A, Strauss LG, Schwarzbach M, et al. Dynamic PET 18F-FDG studies in patients with primary and recurrent soft-tissue sarcomas: impact on diagnosis and correlation with grading. *J Nucl Med* 2001;**42**(5):713–20.
  72. Pope WB, Lai A, Mehta R, et al. Apparent diffusion coefficient histogram analysis stratifies progression-free survival in newly diagnosed bevacizumab-treated glioblastoma. *AJNR Am J Neuroradiol* 2011;**32**(5):882–9, Controlled Clinical Trial Research Support, Non-US Gov't.
  73. Hamstra DA, Chenevert TL, Moffat BA, et al. Evaluation of the functional diffusion map as an early biomarker of time-to-progression and overall survival in high-grade glioma. *Proc Natl Acad Sci USA* 2005;**102**(46):16759–64, Research Support, N.I.H., Extramural Research Support, Non-US Gov't.
  74. Hamstra DA, Rehemtulla A, Ross BD. Diffusion magnetic resonance imaging: a biomarker for treatment response in oncology. *J Clin Oncol* 2007;**25**(26):4104–9, Research Support, N.I.H., Extramural Review.
  75. Moffat BA, Chenevert TL, Lawrence TS, et al. Functional diffusion map: a noninvasive MRI biomarker for early stratification of clinical brain tumour response. *Proc Natl Acad Sci USA* 2005;**102**(15):5524–9, Clinical Trial Research Support, N.I.H., Extramural Research Support, Non-US Gov't Research Support, US Gov't, P.H.S.
  76. Marugami N, Tanaka T, Kitano S, et al. Early detection of therapeutic response to hepatic arterial infusion chemotherapy of liver metastases from colorectal cancer using diffusion-weighted MR imaging. *Cardiovasc Intervent Radiol* 2009;**32**(4):638–46.
  77. Cao K, Gao M, Sun YS, Li YL, Sun Y, et al. Apparent diffusion coefficient of diffusion weighted MRI in endometrial carcinoma-Relationship with local invasiveness. *Eur J Radiol*: Gao YN; 2011.
  78. Simpson-Herren L, Noker PE, Wagoner SD. Variability of tumour response to chemotherapy II Contribution of tumour heterogeneity. *Cancer Chemother Pharmacol* 1988;**22**(2):131–6.
  79. Giesel FL, Bischoff H, von Tengg-Kobligh H, et al. Dynamic contrast-enhanced MRI of malignant pleural mesothelioma: a feasibility study of noninvasive assessment, therapeutic follow-up, and possible predictor of improved outcome. *Chest* 2006;**129**(6):1570–6, Clinical Trial.
  80. Mills SJ, Patankar TA, Haroon HA, et al. Do cerebral blood volume and contrast transfer coefficient predict prognosis in human glioma? *AJNR Am J Neuroradiol* 2006;**27**(4):853–8.
  81. Galban CJ, Chenevert TL, Meyer CR, et al. The parametric response map is an imaging biomarker for early cancer treatment outcome. *Nat Med* 2009;**15**(5):572–6, Research Support, N.I.H., Extramural.
  82. Chang YC, Huang CS, Liu YJ, et al. Angiogenic response of locally advanced breast cancer to neoadjuvant chemotherapy evaluated with parametric histogram from dynamic contrast-enhanced MRI. *Phys Med Biol* 2004;**49**(16):3593–602, Research Support, Non-US Gov't.
  83. Johansen R, Jensen LR, Rydland J, et al. Predicting survival and early clinical response to primary chemotherapy for patients with locally advanced breast cancer using DCE-MRI. *J Magn Reson Imaging* 2009;**29**(6):1300–7, Randomised Controlled Trial.
  84. Padhani AR, Hayes C, Assersohn L, et al. Prediction of clinicopathologic response of breast cancer to primary chemotherapy at contrast-enhanced MR imaging: initial clinical results. *Radiology* 2006;**239**(2):361–74, Research Support, Non-US Gov't.
  85. Yuh WT, Mayr NA, Jarjoura D, et al. Predicting control of primary tumour and survival by DCE MRI during early therapy in cervical cancer. *Invest Radiol* 2009;**44**(6):343–50, Research Support, N.I.H., Extramural.
  86. Thompson G, Mills SJ, Stivaros SM, Jackson A. Imaging of brain tumours: perfusion/permeability. *Neuroimaging Clin N Am* 2010;**20**(3):337–53, Review.
  87. Caseiras GB, Chheang S, Babb J, et al. Relative cerebral blood volume measurements of low-grade gliomas predict patient outcome in a multi-institution setting. *Eur J Radiol* 2010;**73**(2): 215–20, Multicentre Study.
  88. Toma-Dasu I, Uhrdin J, Antonovic L, et al. Dose prescription and treatment planning based on FMISO-PET hypoxia. *Acta Oncologica* 2011, in press. doi:10.3109/0284186X.2011.599815.